JOURNAL OF MATERIALS SCIENCE 23 (1988) 438–450

Ultrasonic relaxation in $CoO–P_2O_5$ glasses at high temperatures

B. BRIDGE, A. A. HIGAZY
Physics Department, Brunel University, Kingston Lane, Uxbridge, Middlesex UB8 3PH, UK

The attenuation of ultrasonic compressional waves in $CoO–P_2O_5$ glasses has been measured over the temperature and frequency ranges 250 to 640 K and 15 to 75 MHz, respectively. Twin loss peaks in the attenuation against temperature plots at constant frequency, were attributed to a relaxation loss of the standard linear solid type, with low dispersion and two, discrete, Arrhenius relaxation times. Unlike the case of low-temperature loss peaks in glasses, it was not found necessary to assume a continuum of relaxation times to explain the width of the loss peaks. Activation energies and attempt frequencies were in the range, respectively, almost one and three orders of magnitude higher than corresponding values typifying the low-temperature loss peaks in the same glass system. This result suggests the existence of 2-well systems with dimensions of the order of the diameter of a structural unit or atomic ring rather than the width of one or two atoms, and perhaps relaxing particles the size of a structural unit rather than a single oxygen atom. Activation energies in the various glasses were found to be proportional to the product of the mean force constant and compressibility. The calculated number of two-well systems (loss centres) per unit volume is small and comparable with what obtains in the low-temperature loss case. The composition dependence of several other properties of the relaxation process is discussed and a common feature is a discontinuity in the composition dependence of all of these properties at metaphosphate composition.

1. Introduction

Ultrasonic relaxation phenomena in oxide glasses have been widely studied below room temperature. Investigations at elevated temperatures up to the softening point are rare and the present paper gives the first published data on phosphate glasses. At a constant frequency, peaks in the temperature dependence of the attenuation occur which seem attributable to a standard linear solid behaviour with low dispersion and Arrhenius relaxation times. Whilst differing from the low-temperature relaxation loss in terms of the order of magnitude of the activation energies and attempt frequencies characterizing the loss, the most interesting feature of the high relaxation phenomenon is the width of the loss peaks, each of which can be understood in terms of the operation of a single relaxation time, i.e. there exist discrete relaxation spectra. A stumbling block in understanding low-temperature relaxational phenomena in glasses is the difficulty in obtaining a unique [1–4] continuum relaxation spectrum (relaxation strength–relaxation time plot) to fit the broad peaks observed. Relaxation strengths should be unambiguously assignable to the high-temperature peaks and prospects for theoretical interpretation of the observations ought to be enhanced, correspondingly.

2. Experimental procedure

The specimen holder for the high-temperature measurements is illustrated in Fig. 1. This holder was designed to aid the production of exponentially decaying echoes, by means of a device which allowed the contact pressure on the crystal–bond–specimen combination to be varied. This pressure, which was always slight to prevent transducer breakage, was applied by means of a spring which, via a ball and socket joint, engaged a contact button resting on the transducer. It could be finely controlled by means of a continuously adjustable clamp, consisting of a large nut on the threader bar which carried the spring and the ball and socket joint. These springs also cushioned the effect brought about by differential thermal contraction or expansion of the sample and the sample holder. All electrically insulating parts of the sample holder (for example, the collars for the rods supporting the contact buttons) were made of asbestos to permit high-temperature operation.

After obtaining the best exponential echo pattern at room temperature, the holder was mounted centrally in a cylindrical furnace of dimensions 17 cm diameter and 30 cm long. A heat-resistant cable (extending 30 cm outside the furnace) connected the transducer to conventional 50 Ω cable. The special cable consisted of an outer conducting rod of german silver (0.1 cm diameter), separated from an inner copper conductor (1 mm diameter) by means of an alumina tube (see Fig. 1). (The german silver rod was soldered on to the end of the brass tube illustrated in Fig. 1, whilst the inner conductor was soldered directly on to the brass contact button located concentrically in the brass tube.) The furnace temperature was controllable from room temperature to 900 K by means of a

0022–2461/88 $03.00 + .12

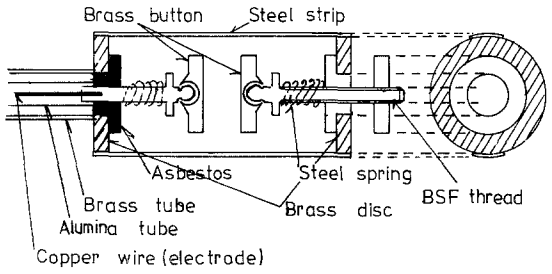

Figure 1 Specimen holder for ultrasonic wave attenuation and velocity measurements at high temperatures. The ball and socket joints allow ready variation of contact pressure to be made, in order to obtain exponentially decaying echoes.

temperature controller (Transitrol Ether). Temperatures were measured by means of a digital thermometer (Comark Type 5000) and a chromel–alumel thermocouple in contact with the middle of the glass rods. The thermocouple leads were protected by alumina sleeves.

Ultrasonic wave transit time and the acoustic loss were measured at 10 K intervals, increasing from room temperature to 650 K, with the help of a temperature controller (measurements could not be performed at temperatures $\geqslant 650$ K because deterioration of the bond rendered the measurement accuracy too poor for present purposes). However, in any event it could not have been possible to proceed to much higher temperatures as the glass started to soften rapidly at ~ 680 K.

A 15 MHz quartz X-cut transducer was employed as a common transmitter/receiver. Pulse-echo equipment, including an automatic attenuation recorder, was supplied by Matec Inc., and the circuit and measurement technique was as described previously [2]. Transit time measurements were made by the pulse-echo overlap technique [5] employing the use of a high-resolution frequency source (Matec model 110), decade dividers, dual delay generators (Matec model 122B), and a high-stability frequency counter (Racal-Dana 9914) in conjunction with the pulse-echo equipment just described.

A considerable amount of research was carried out to find an appropriate coupling fluid to make acoustic bonds withstand the temperature range 300 to 650 K. Of several materials tried, best echo patterns were obtained using 0V-25, a silicon-based grease chemically described as a gas chromatography stationary phase, supplied by J.J. Chromatographic Ltd.

The seven glasses selected for the study were the same as those used in the low-temperature measurement described previously [1, 2].

3. Results and computer fit to twin single relaxation processes

We shall deal only with the absorption measurements on the grounds of space. Velocity measurements are to be dealt with in a separate publication for direct comparison with low-temperature velocity data.

Typical results showing the temperature dependence of the absorption at ~ 15 to 75 MHz are illustrated by data points given in Figs 2a to g for all Co–P–O glasses of different compositions. From inspection of these figures we observed that for any glass composition two loss peaks are obtained, which we shall label R_1 and R_2, for the lower and high peak temperatures, respectively. As these peaks shifted to higher temperatures with increasing frequency, it is natural to attempt an interpretation of these losses in terms of a relaxation-type process with a loss maximum occurring at $\omega\tau = 1$ where ω is the angular frequency and τ is the relaxation time (for example as in Voigt or standard linear solid type behaviour) and "thermally activated relaxation time" of the form

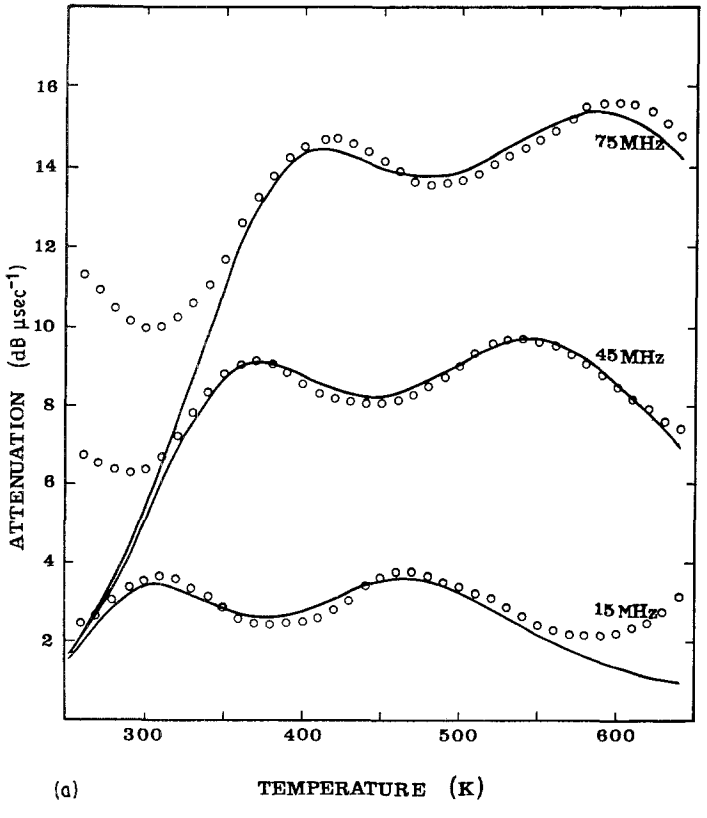

Figure 2 (a) to (g) Temperature dependence of the attenuation of longitudinal acoustic waves in CoO_3–P_2O_5 glasses in the temperature and frequency ranges 250 to 650 K and 15 to 75 MHz. (o) Experimental data points, (——) theoretical fit to a relaxation process of a standard linear form, with low dispersion, with two discrete Arrhenius relaxation times and relaxation strengths proportional to reciprocal temperature. (a) 7.6 mol % CoO, (b) 20 mol % CoO, (c) 35 mol % CoO, (d) 42.4 mol % CoO, (e) 47 mol % CoO, (f) 49.4 mol % CoO, (g) 54.3 mol % CoO.

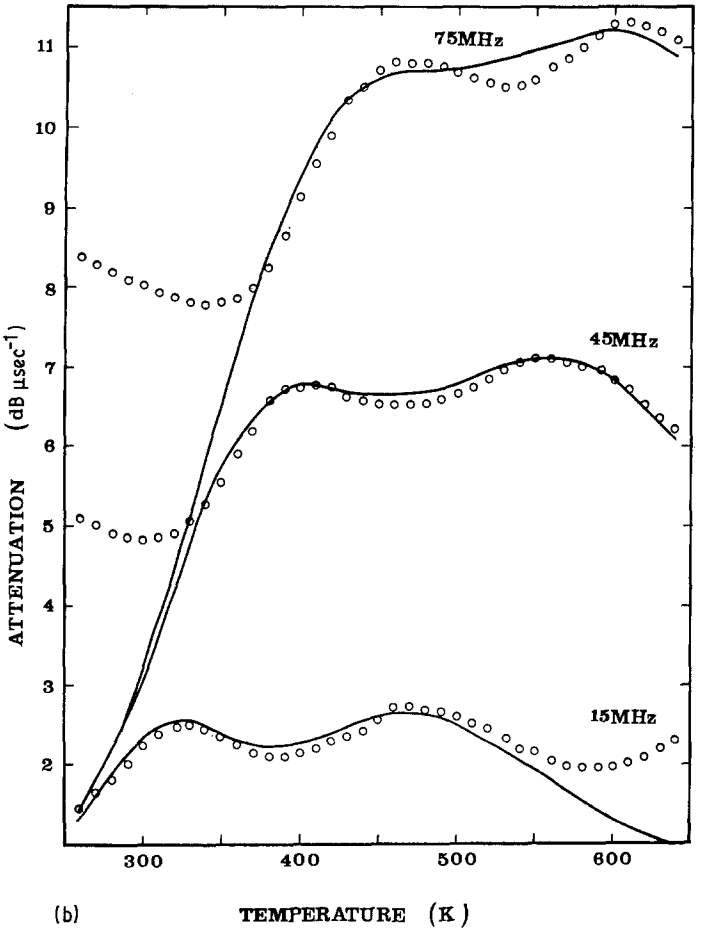

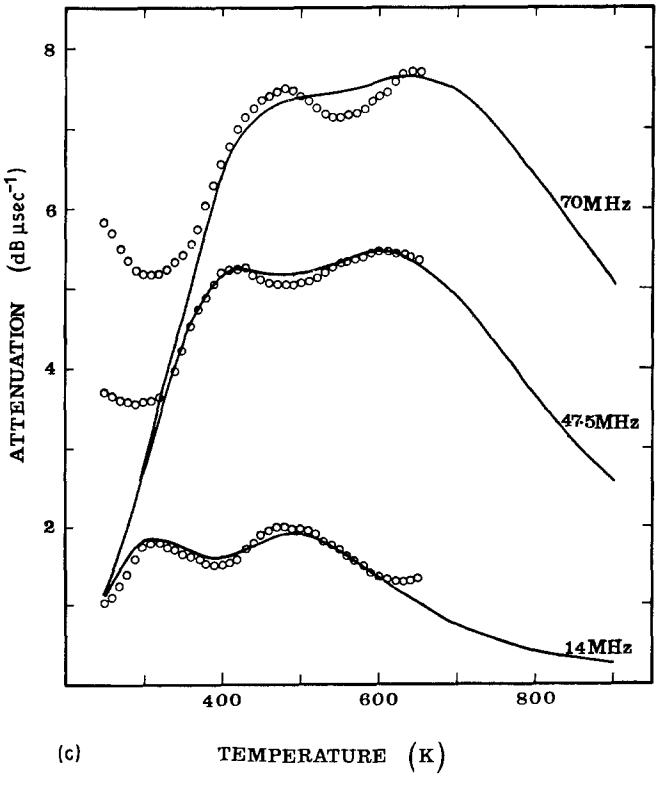

Figure 2 Continued.

$\tau = \tau_0 e^{V/kT}$. Further, the relatively small change of velocity with temperature at elevated temperatures (to be discussed in a separate publication) suggests a loss of the standard linear solid type, with low dispersion (Equation 1 of [2]). This shift in peak temperature for a given frequency change is large compared with that associated with the peak occurring at less than 300 K (at about liquid nitrogen temperatures) discussed elsewhere [2]. For example, specimen a_2 (20.0 mol % CoO) shows a shift in peak temperature (taking, for example, the absorption peak R_1) from 325 K at 15 MHz to 460 K at 75 MHz. The attenuation, especially at the peak temperature, increases rapidly with the frequency, and thus limited our measurements to $\leqslant 75$ MHz.

Values of attempt frequency ($\nu_0 = 1/\tau_0$) and the average activation energy V of the process, R_1 and R_2

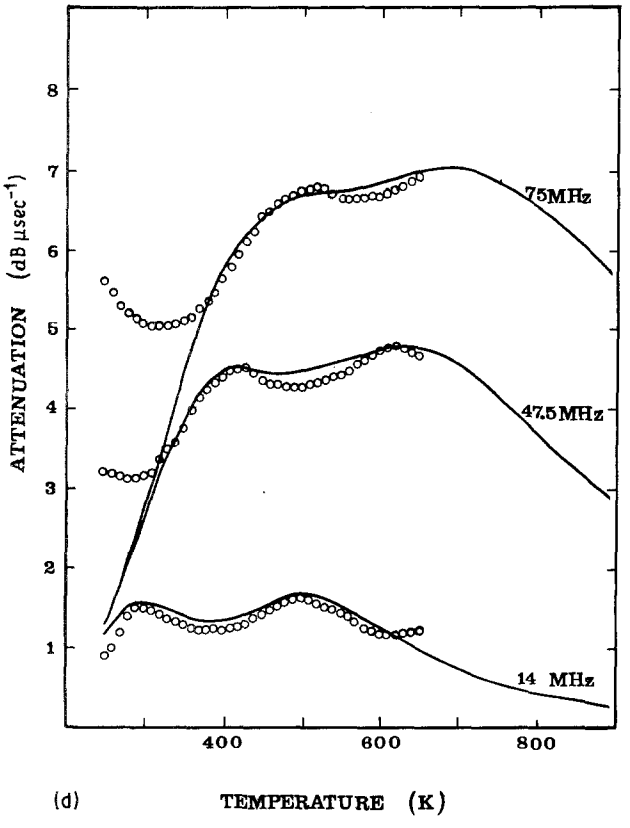

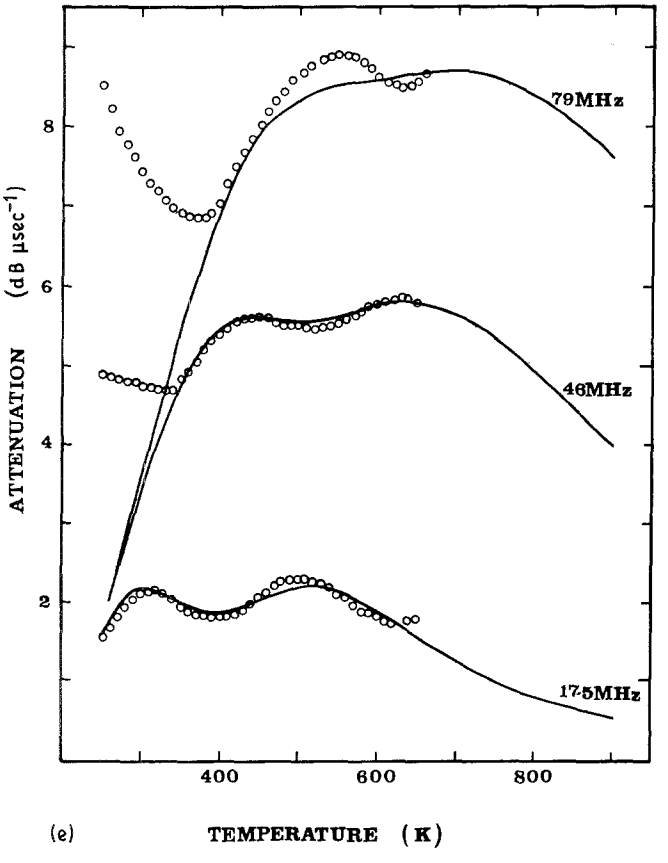

Figure 2 Continued.

were obtained from the intercept and the slope of the graph log ω against $1/T_p$ (Figs 3a to d, respectively). The values of the attempt frequency obtained (Table I) are of the order of 10^{10} Hz, much lower than the values found in low-temperature relaxation processes ($\sim 10^{13}$ Hz).

A straight line in Figs 3a to d, i.e. the graph of log ω against T_p^{-1}, confirms that the strong absorption peaks R_1 and R_2 are indeed consistent with a standard linear solid with low dispersion. Further, from inspection of the experimental width of R_1 and R_2 peaks (Figs 2a to g) we note that a single relaxation time approximation can be admitted. Assuming symmetric wells [1] for simplicity,

for R_1 process

$$Q^{-1} = \frac{\text{const}_1}{kT} \frac{\omega\tau_{01} e^{V_1/kT}}{1 + \omega^2\tau_{01}^2 e^{2V_1/kT}} \quad (1)$$

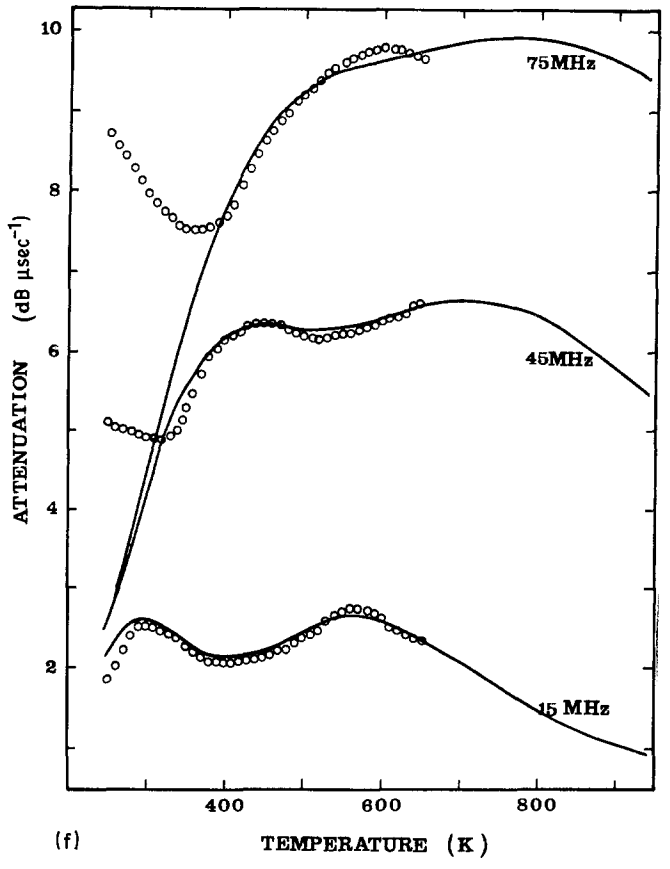

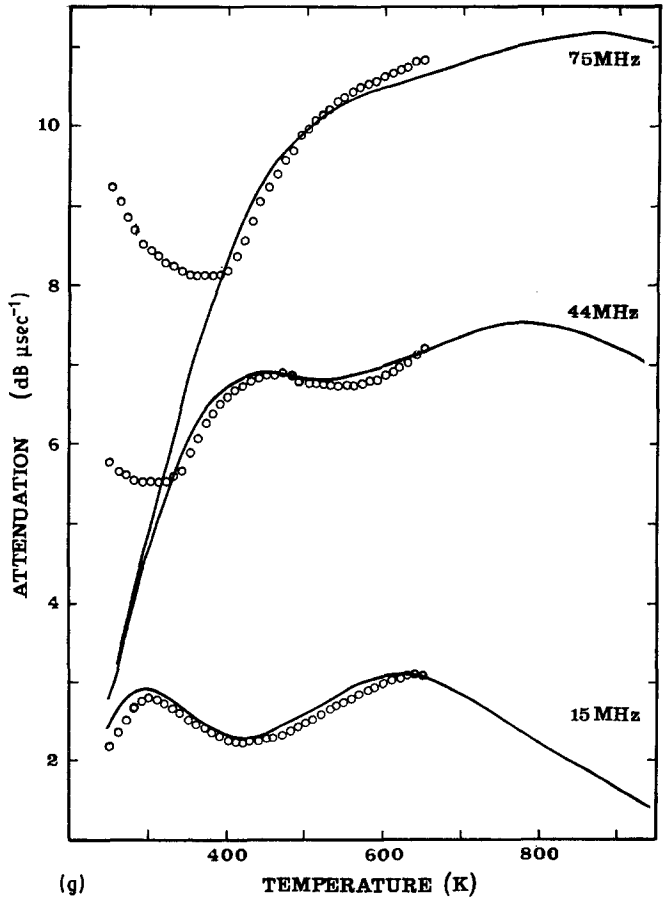

Figure 2 Continued.

for R_2 process

$$Q^{-1} = \frac{\text{const}_2}{kT} \frac{\omega\tau_{02} e^{V_2/kT}}{1 + \omega^2\tau_{02}^2 e^{2V_2/kT}} \quad (2)$$

where Q^{-1} equals internal friction.

So we attempt a theoretical fit to our attenuation data by computer programming, using the following summation of the R_1 and R_2 single relaxation processes

$$Q^{-1} = \frac{C_1}{kT} \frac{\omega\tau_{01} e^{V_1/kT}}{1 + \omega^2\tau_{01}^2 e^{2V_1/kT}} + \frac{C_2}{kT} \frac{\omega\tau_{02} e^{V_2/kT}}{1 + \omega^2\tau_{02}^2 e^{2V_2/kT}} \quad (3)$$

TABLE I Summary of high-temperature ultrasonic properties of cobalt–phosphorus glasses

Glass no.	CoO + Co_2O_3 (mol %)	Density ($g\,cm^{-3}$)	Peak temperature (K)	Peak loss ($dB\,\mu sec^{-1}$)	Frequency (MHz)	Attempt freq. (10^{10} Hz)		Activation Eng. (eV)		Potential well width, L, using m = oxygen mass (nm)	Potential well width, L, using m = structural unit mass (nm)	Relaxation strength, C ($\times 10^{-5}$ eV)	Number of loss centres per cm^3. $n_1 \times 10^{20}$	Number of loss centres as a fraction of oxygen density
						Starting value	Values used for computer fit	Starting value	Values used for computer fit					
Relaxation process R_1														
a_1	7.6	2.685	370	9.10	45.0	1.3800	1.3473	0.175	0.182	0.475	0.161	42.00	12.18	2.21
a_2	20.0	2.845	410	6.75	45.0	0.3880	0.2988	0.145	0.148	0.896	0.312	30.73	11.07	2.02
a_3	35.0	2.892	430	5.25	47.5	0.1060	0.1159	0.121	0.117	1.715	0.625	23.31	9.56	1.87
a_4	42.4	2.914	435	4.50	47.5	0.0704	0.0797	0.103	0.105	2.104	0.786	19.89	9.16	1.80
b_1	47.0	2.985	448	5.59	45.0	0.0523	0.0513	0.090	0.094	2.441	0.928	25.25	13.16	2.59
b_2	49.4	3.013	460	6.34	45.5	0.0419	0.0364	0.083	0.083	2.728	1.045	43.10	24.17	4.75
b_3	54.3	3.133	470	6.88	45.0	0.0303	0.312	0.075	0.077	3.207	1.249	49.61	32.51	5.37
Relaxation process R_2														
a_1	7.6	2.685	540	9.70	45	1.9483	2.448	0.273	0.293	0.400	–	64.0	13.80	2.50
a_2	20.0	2.845	550	7.10	45	1.7870	1.901	0.267	0.286	0.418	–	45.62	10.94	1.99
a_3	35.0	2.892	600	5.47	47.5	0.6846	0.9270	0.257	0.273	0.675	–	35.89	8.91	1.74
a_4	42.4	2.914	620	4.80	47.5	0.4781	0.729	0.246	0.269	0.808	–	33.44	8.62	1.70
b_1	47.0	2.985	630	5.87	45.0	0.3983	0.7931	0.243	0.279	0.885	–	40.35	10.85	2.13
b_2	49.4	3.013	710*	6.65	45.5	–	0.534*	–	0.287*		–	56.0*	15.39	3.02
b_3	54.3	3.133	790*	7.55	45.0	–	0.4053*	–	0.302*		–	74.00*	22.33	4.38

*Theoretical values. These peaks are outside the range of the experimental data and have been derived from the computer fit using the liberated values of attempt frequency and activation energy.

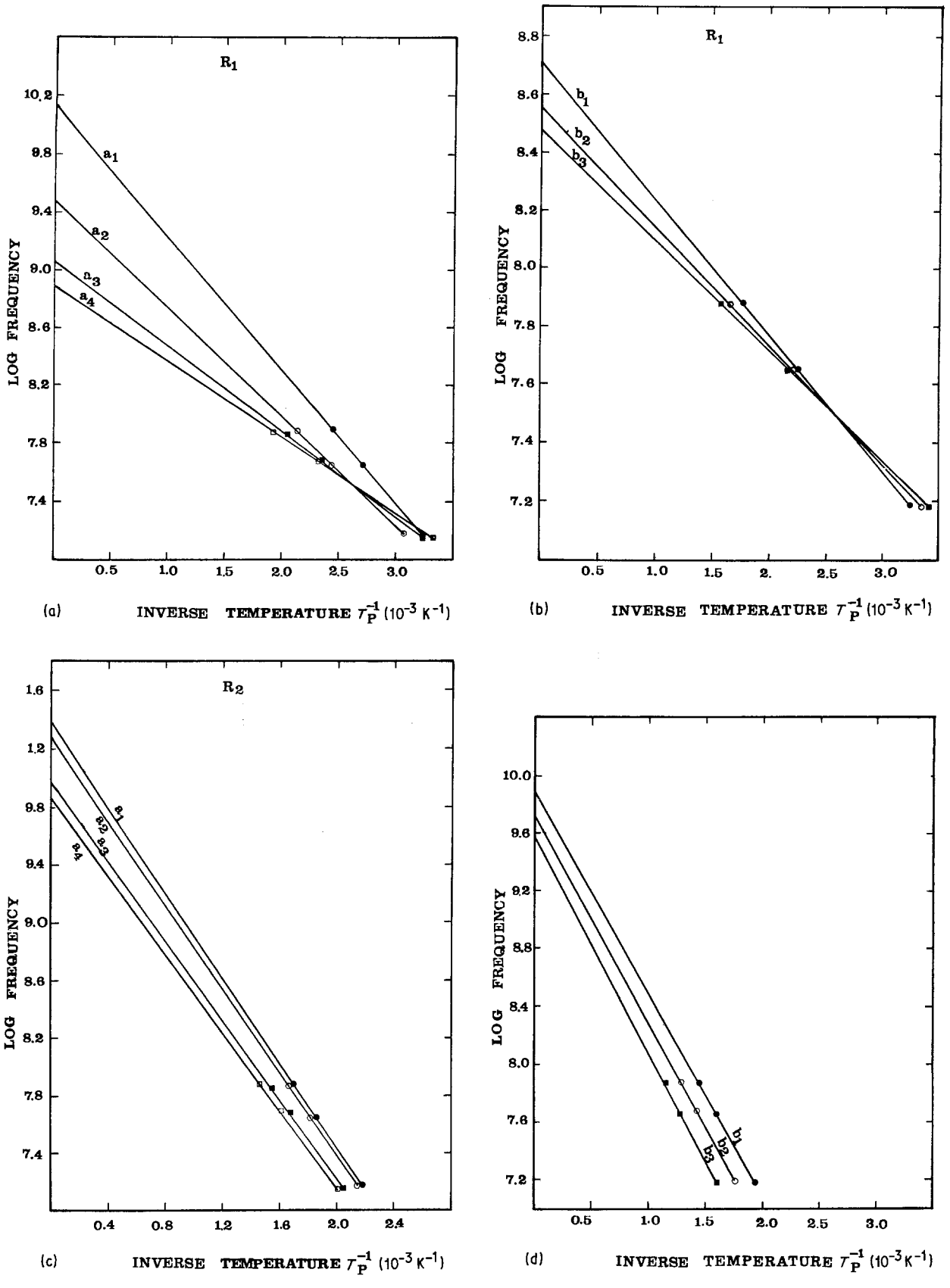

Figure 3 (□, ■, ○, ●) The relationship between the temperature of the attenuation peaks shown in Fig. 2 and frequency. (——) Regression lines obtained from the Arrhenious equation $\omega\tau_0 \exp(V/kT_p) = 1$, with the notation as defined in the text. R_1 and R_2 denote the lowest and highest peak temperatures, respectively. a_1, 7.6 mol % CoO; a_2, 20.0 mol % CoO; a_3, 35.0 mol % CoO; a_4, 42.0 mol % CoO. b_1, 47.0 mol % CoO; b_2, 49.4 mol % CoO; b_3, 54.3 mol % CoO. For the R_2 peaks in samples b_2 and b_3 the peak temperatures are theoretical values obtained from the computer fit, the peaks lying outside the range of experimental data.

Now to obtain the values of C_1, C_2, τ_{01}, τ_{02}, V_1 and V_2 which give the best fit of Q^{-1} to our data over all the temperature range, we first calculate the values of C_1 and C_2 by substituting as "starting values" the quantities V_1, V_2, τ_{01} and τ_{02} obtained from the slope and the intercept of the graph $\log \omega$ against $1/T_p$, respectively (see Figs 3a to d), into the following equations at 45 MHz. Then we used a computer program to solve the following simultaneous equations for C_1 and C_2

$$Q_{P1}^{-1} = \frac{C_1}{kT_{P1}} \frac{\omega\tau_{01} e^{V_1/kT_{P1}}}{1 + \omega^2\tau_{01}^2 e^{2V_1/kT_{P1}}} + \frac{C_2}{kT_{P1}} \frac{\omega\tau_{01} e^{V_2/kT_{P1}}}{1 + \omega^2\tau_{01}^2 e^{2V_2/kT_{P1}}} \quad (4)$$

$$Q_{P2}^{-1} = \frac{C_1}{kT_{P2}} \frac{\omega\tau_{02} e^{V_1/kT_{P2}}}{1 + \omega^2\tau_{02}^2 e^{2V_1/kT_{P2}}} + \frac{C_2}{kT_{P2}} \frac{\omega\tau_{02} e^{V_2/kT_{P2}}}{1 + \omega^2\tau_{02}^2 e^{2V_2/kT_{P2}}} \quad (5)$$

where Q_{P1}^{-1} and Q_{P2}^{-1} are the experimental internal frictions at the peak temperatures T_{P1} and T_{P2}, respectively. Then, substituting the values of C_1, C_2 obtained, and the "starting values" V_1, V_2, τ_{01} and τ_{02} into Equation 3 at different temperature values in 10 K intervals, we found that these values did not give a good fit, i.e. the trough between maxima was usually absent, and the Q^{-1} value regenerated from these values decreased very rapidly at high temperature. So to reproduce the trough between maxima, the value of τ_{01} was increased from the starting value (τ_{02}, V_1 and V_2 are fixed at their starting values). Then the value of τ_{02} was decreased from the starting value (the new value of τ_{01} and the starting values of V_1 and V_2 remaining fixed) to reproduce the experimental value of Q^{-1} at high temperatures (i.e. higher than the position of the second peak). However, these adjustments caused slight shifts in the peak temperatures T_{P1} and T_{P2} towards the low temperature (the peak heights remained relatively unaffected). So by increasing the values of V_1 and V_2 from the starting values (τ_{01} and τ_{02} remaining fixed at their new values) the computer-reproduced peak temperatures T_{P1} and T_{P2} were thus brought into agreement with their experimental values. The final set of V_1, V_2, τ_{01} and τ_{02}, in addition to the obtained values of C_1 and C_2 at about 45 MHz for each glass give a close fit (solid lines) to the experimental absorption data (full circles) at all other frequencies (see Figs 2 to 8).

4. Compositional dependence of the high-temperature acoustic loss of Co–O–P glasses

Fig. 4 shows that the average activation energy (obtained from the peak shift, Figs 9 to 12) decreased with cobalt oxide content, and ranges from 0.08 to 0.18 eV for the relaxation process R_1 and from 0.24 to 0.27 eV for the relaxation process R_2. These energy values are much higher than found in low-temperature relaxation processes (see Table I).

As mentioned before in Section 3, to obtain a good fit to our data (using computer programming) the starting V and τ_0 values are changed. These values of V and τ_0 used in the computer fit are given in Table I, together with the starting V and τ_0 values. In the case of the R_1 process, the variations of the activation energy, used in computer programming, and the starting values of V with composition take the same form (see Figs 4b and 5b). However, in the case of the R_1 process it will be observed that there is a quite close agreement between the two values of V in the range

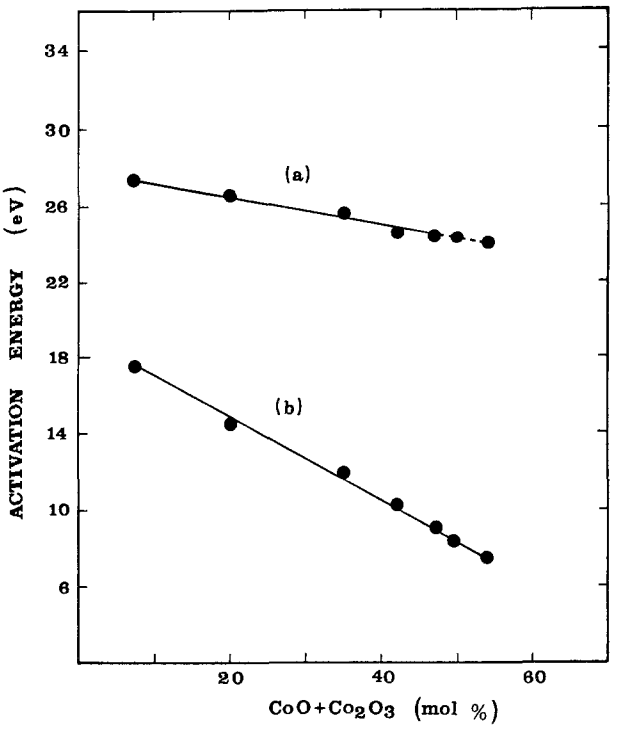

Figure 4 Composition dependence of the activation energies derived by applying the Arrhenius equation $\omega\tau_0 \exp(V/kT_P) = 1$, to the loss peaks (b) R_1 and (a) R_2. (See Fig. 3.)

0 to 42 mol %; but moving towards 60 mol % CoO, the experimental V values continuously decreased, while the other (i.e. the value of V used in computer programming) shows an increase (see Figs 4a and 5a).

Figs 6, 7 and 8 show that the peak loss, peak temperature and the relaxation strength are quite sensitive

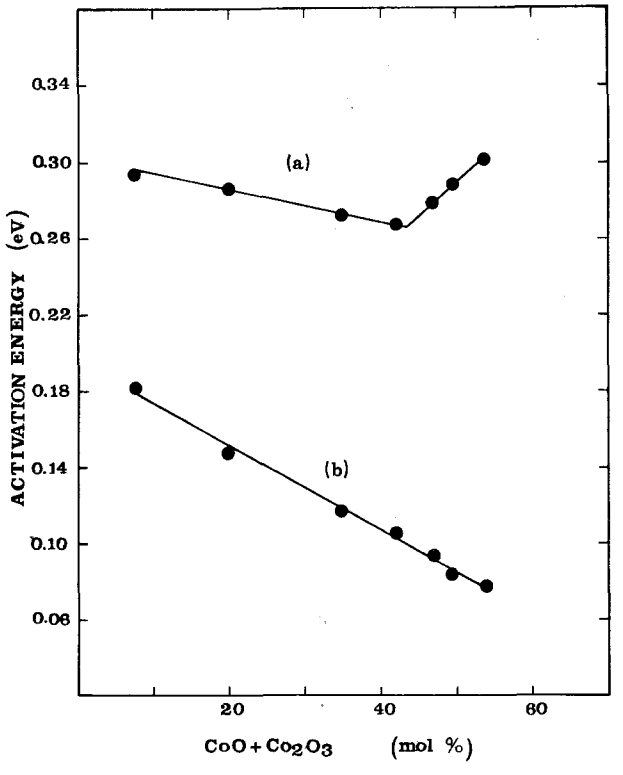

Figure 5 Composition dependence of the activation energies used in the theoretical fit of the shapes of the overlapping loss peaks (b) R_1 and (a) R_2 to a relaxation process of a standard linear solid form, with two discrete Arrhenius relaxation times and relaxation strengths proportional to reciprocal temperature (solid lines in Fig. 2).

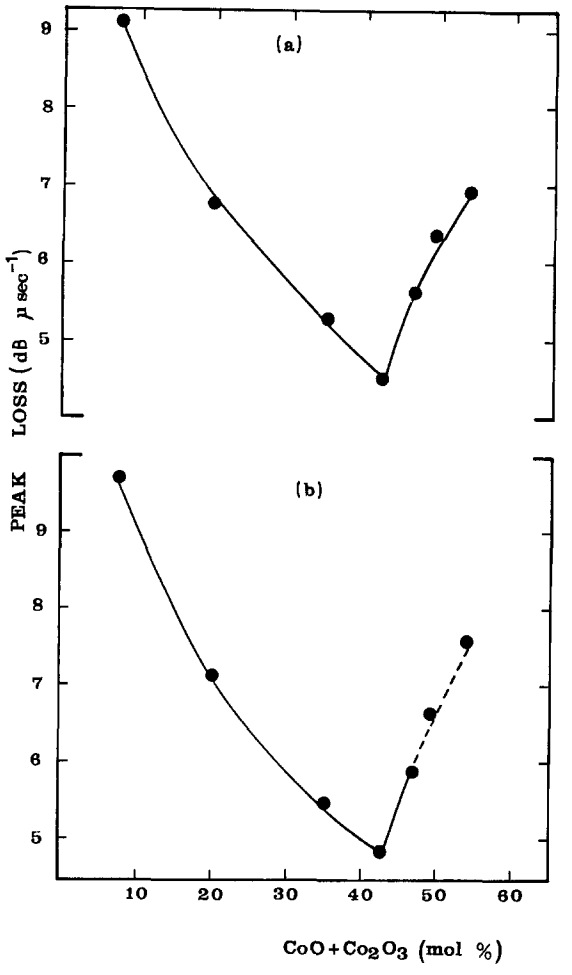

Figure 6 Composition dependence of the acoustic attenuation peaks plotted in Fig. 1. (a) R_1, (b) R_2.

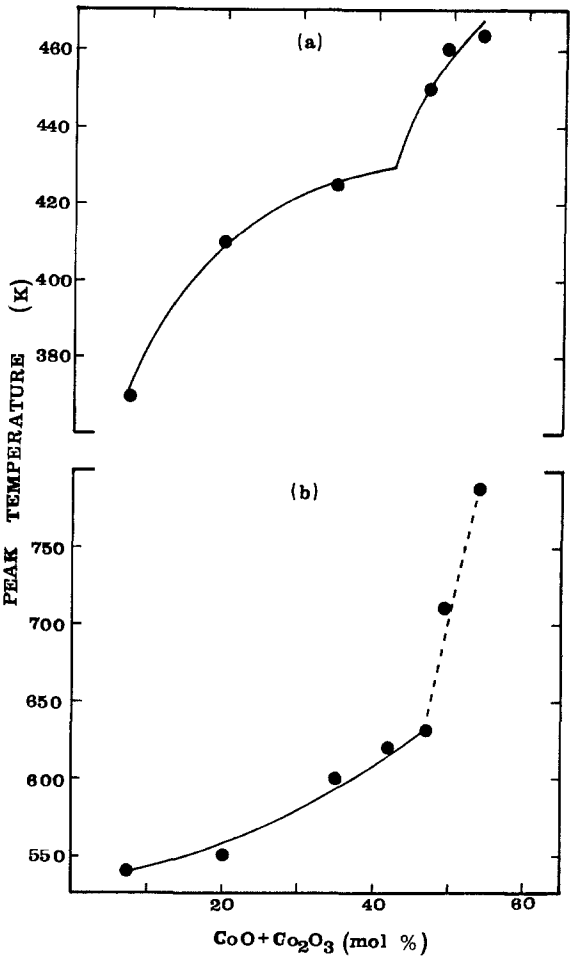

Figure 7 Composition dependence of loss peak temperatures. (a) R_1, (b) R_2.

to composition, i.e. exhibit the same "discontinuity" at ~42 mol % CoO that we have found in the composition gradients of other physical properties of these glasses [6, 7]. In contrast, the attempt frequency, ν_0, is a monotonically decreasing function of the CoO mol %, displaying no evidence of discontinuities (see Fig. 9).

5. Physical interpretation

We have shown that there are two thermally activated relaxation processes of activation energies ~0.1 to 0.3 eV governing the acoustic loss in Co–P–O glasses in the temperature range from 300 to 650 K. Thus we suggest that the loss originates from particles in two-well systems, like the low-temperature loss. However, the barrier heights are substantially higher and the attempt frequencies much lower than those obtaining in the low-temperature case. The magnitude of the attempt frequencies is particularly illuminating for it suggests particle motions in wells substantially greater than the average interatomic spacing and/or particle masses substantially larger than those responsible for the low-temperature behaviour. To quantify these suggestions, let us consider the simplest model of a particle in a flat-bottomed vertical sided, double-well potential, the width of either well being L. If we interpret the attempt frequency ν_0 as the classical vibrational frequency of the particle, and assume that the particle is in the ground state, we have

$$h\nu_0 = h^2/8mL^2 \qquad (6)$$

where h is Planck's constant and m is the particle mass. (In the detailed theory in the Appendix to [2], ν_0 is twice the classical vibration frequency of the particle in either well, increasing all values of L predicted in this paper by a factor $2^{1/2}$.)

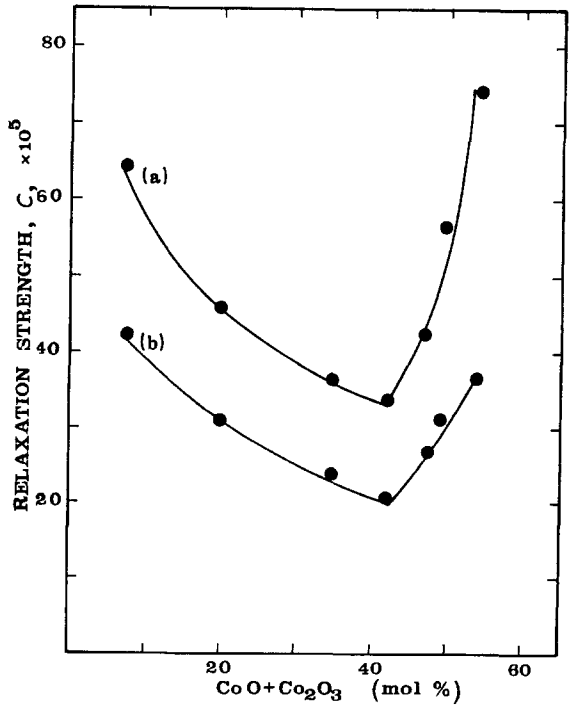

Figure 8 Composition dependence of the relaxation strengths used in the computer fit described in the text and in the captions to Figs 2 and 5. (a) R_2, (b) R_1.

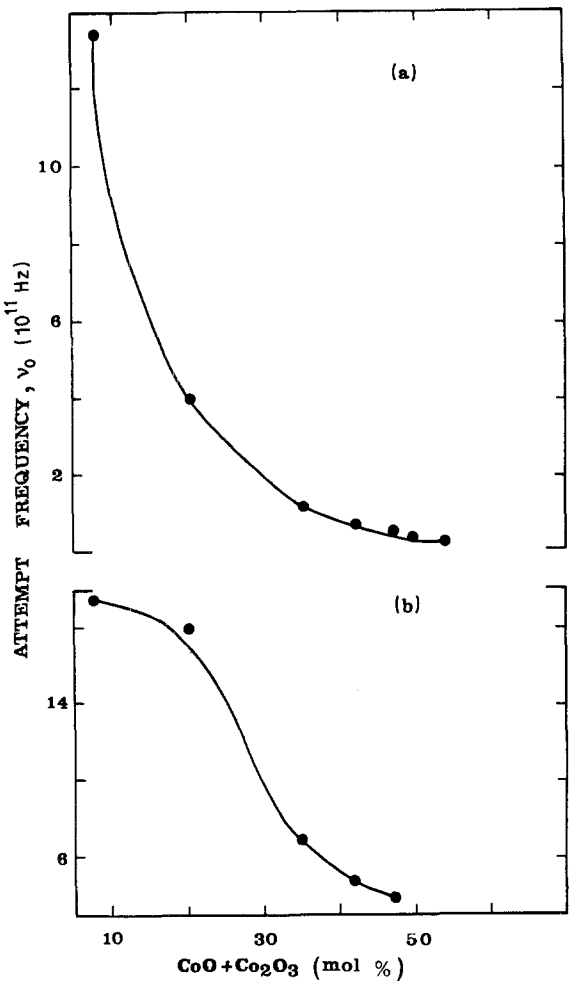

Figure 9 Composition dependence of the attempt frequencies τ_0^{-1} obtained from the regression lines to $\omega\tau_0 \exp(V/kT_p) = 1$, plotted in Fig. 3.

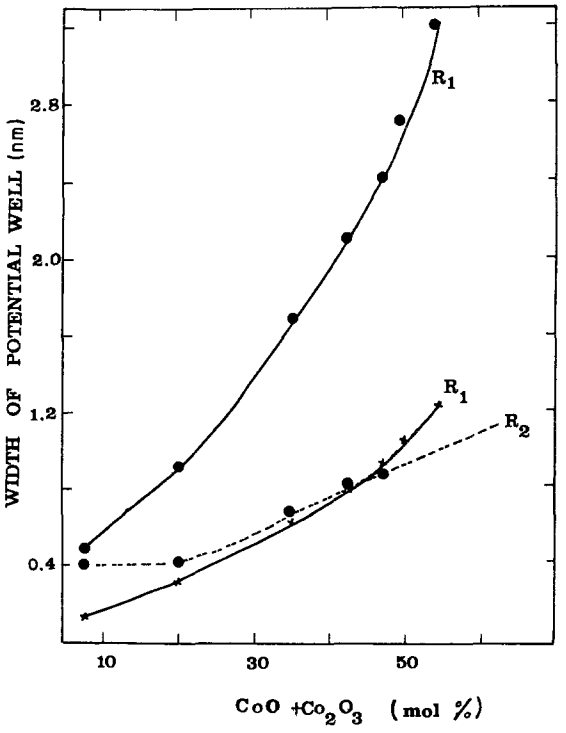

Figure 10 Composition dependence of the width of potential wells, L, arising from the assumption that the attempt frequencies, τ_0^{-1}, calculated from the acoustic attenuation data, derive from ground state vibrations of particles in flat-bottomed wells. (●) Calculated values of L assuming that the mass of the relaxing particle is equal to the mass of an oxygen atom. (x) Values of L obtained if the relaxing particle has the mass of one structural unit of the glasses.

Thus taking for m the mass of the oxygen atom we find that L lies between the limits (Fig. 10) 0.4 and 3.2 nm. Let us suppose that a substantial segment of network, for example a whole structural unit (i.e. the mass of a glass formula unit) vibrates in a two-well potential. (In fact we had in mind the vibration of whole atomic rings, but it is difficult to ascribe a precise mass to an atomic ring throughout our entire glass range; it is, however, of the same order as the glass-formula-unit mass.) We then find that L lies between the limits 0.161 and 1.2 nm, i.e. it is still, in most cases, several interatomic spacings (Fig. 10).

These large values of L draw attention to the existence of two possible interpretations for the high-temperature loss mechanism.

(i) Diffusion of single atoms from ring to ring caused by "holes", i.e. atomic vacancies in the network (see Paths 1, 2 and 3 in Fig. 11). This model works satisfactorily for glasses for CoO content < 20 mol % for which $L \simeq$ a ring diameter. However, for glasses of higher CoO content, one has to assume the atom to jump across several interatomic rings (Path 4), if single atoms were assumed to be the two-well particle. However, because the experimental activation energies are low compared with Co–O and P–O bond strengths, the implication is that atoms which are almost ionized initially (highly distorted bonds) are involved in this diffusion process.

(ii) Diffusion of a structural unit (or some similarly large mass, like one or several atomic rings or ring segments), over a distance which varies from the interatomic distance at low CoO oxide contents to approximately twice the ring diameter distance at high CoO content (see Table I).

In our opinion, however, the observed relaxation processes R_1 and R_2 are not associated with viscous flow, which is characterized by a relatively high activation energy (2–3 eV) and associated with permanent (i.e. irreversible) structural change. The same conclusion could be reached on other grounds when we consider that all the loss processes observed took place below the softening temperature of the glasses.

6. Computation of the number of loss centres

We can estimate the number of loss centres as follows. From previous arguments let us assume [8] that the deformation potential D governing the interaction of

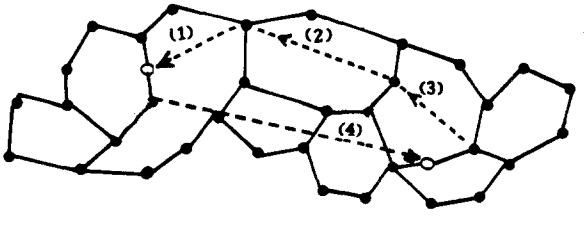

Figure 11 Interpretation of the high-temperature acoustic loss mechanism, showing the diffusion of single atoms from ring to ring (Paths 1, 2, 3) or the hopping across several interatomic rings in a single step (Path 4).

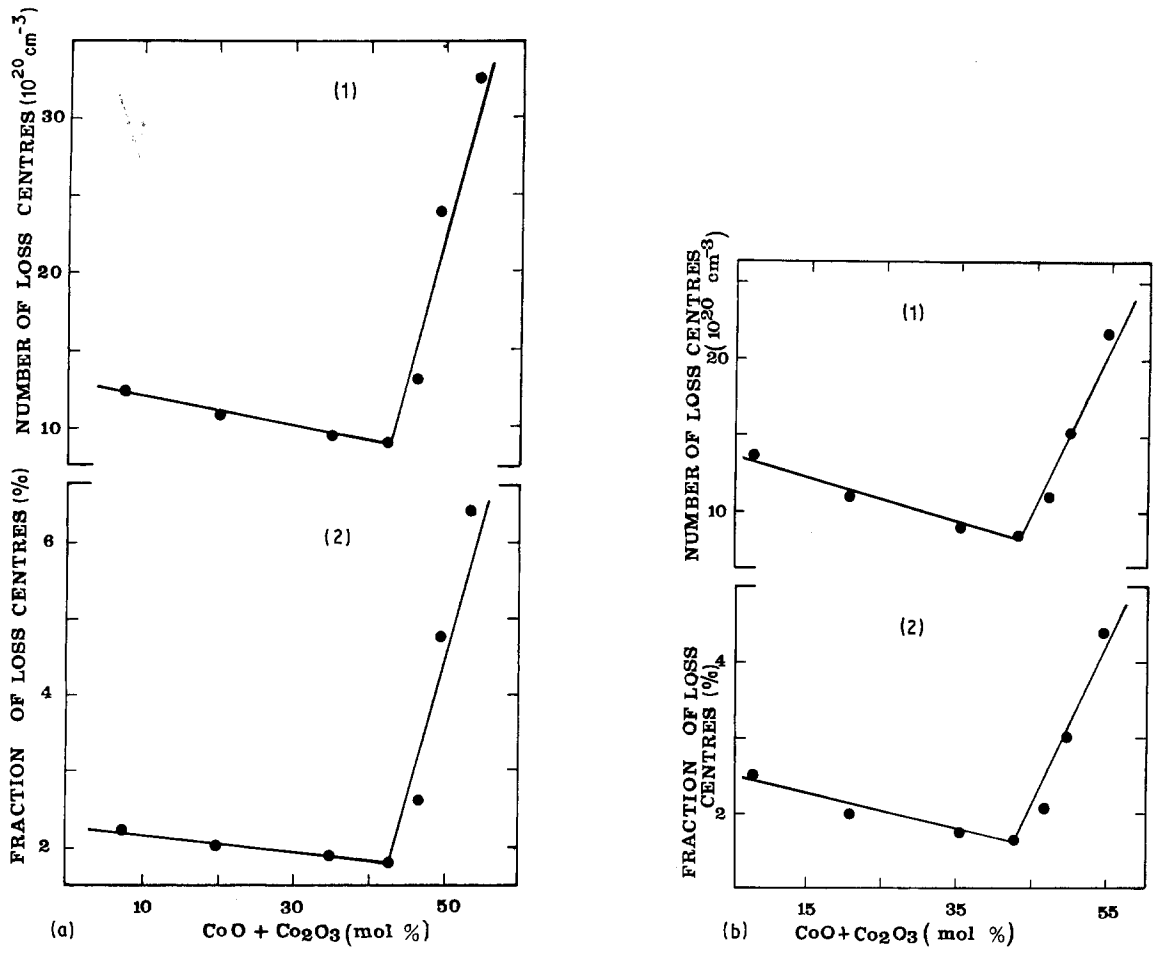

Figure 12 Composition dependence of the number of loss centres (two-well systems) per unit volume and the number expressed as a fraction of the number of oxygen atoms per unit volume in CoO_3–P_2O_5 glasses. (1) R_1 relaxation process, (2) R_2 relaxation process.

compressional waves with a two-well system takes the form

$$D \sim 1.3\,V^{1/3}\ \text{eV} \tag{7}$$

For the R_1 and R_2 processes we have

$$n_1 D^2/4\varrho c_L^2 = C_1, \quad n_2 D^2/4\varrho c_L^2 = C_2 \tag{8}$$

where ϱ is the gloss density and c_L is the compressional wave velocity. Substitute D from Equation 7 into Equation 8 and we find

$$n_1 = 2.37\,\varrho c_L^2 (C_1/V_1^{2/3}) \tag{9}$$

$$n_2 = 2.37\,\varrho c_L^2 (C_2/V_2^{2/3}) \tag{10}$$

The number of loss centres n_1 and n_2 expressed as a fraction of the number of O atoms are given in Table I. Figs 12a and b show the compositional dependence of n_1 and n_2 calculated from Equations 9 and 10. These figures show that these quantities n_1 and n_2 are quite sensitive to composition, i.e. exhibit the same discontinuity at ~43 mol % CoO that we have found in other physical properties of the same glasses.

7. Correlation between the acoustic relaxation loss and elastic properties

By inspection of Figs 6, 8, 12a and 12b we note that the height of the loss peaks are fairly accurately proportional to the relaxation strength, C, and the number of loss centres, n. All these quantities vary in

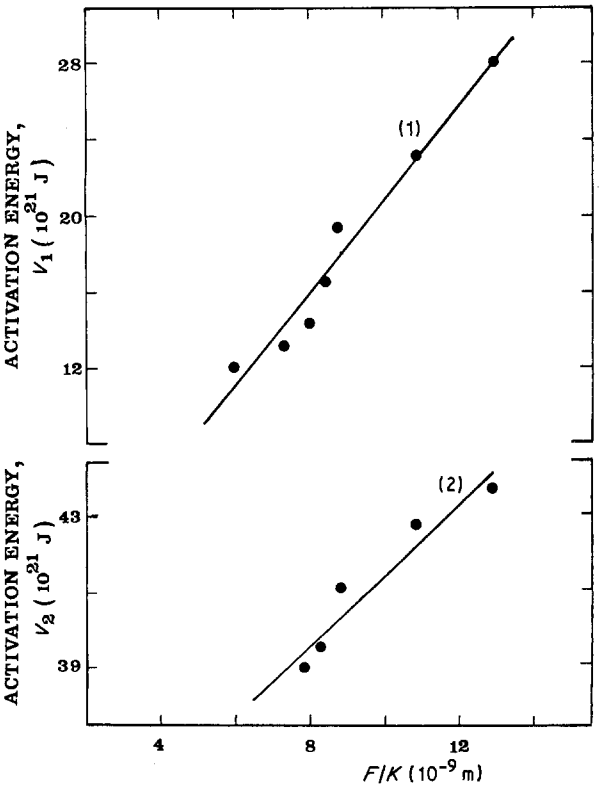

Figure 13 Relationship between activation energies and the product of the mean force constant, F, and compressibility, K, suggested by the model of Bridge and Patel [1, 2, 9]. (●) Experimental data points, (——) least squares linear regression performed on F and F/K. Subscripts to V refer to the R_1 and R_2 processes, respectively.

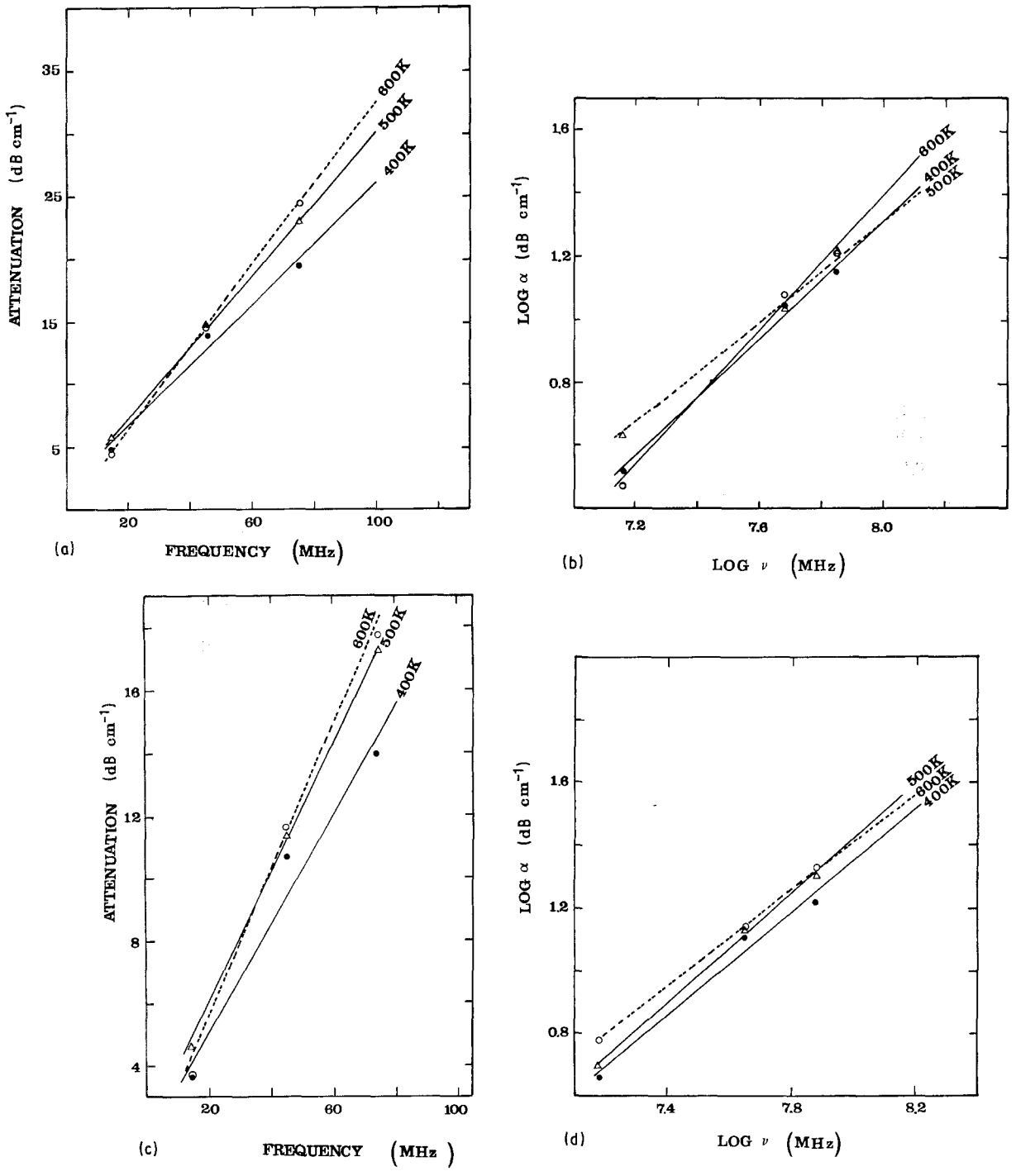

Figure 14 Composition dependence of attenuation against frequency plot at constant temperature. (a) 20 mol % CoO, (b) 35 mol % CoO, (c) 47 mol % CoO, (d) 54.3 mol % CoO.

a similar manner with CoO mol % and display the same discontinuity at ~42 mol % that we have found in the other physical properties of these glasses. In contrast, the activation energy (starting value) is a monotonically decreasing function of the CoO mol % (see Fig. 13).

For the low-temperature multi-relaxational process attributed to an ensemble of two-well systems having a range of barrier heights and perhaps asymmetries, Bridge and Patel [2, 9] proposed a number of simple relationships between the well parameters, the oxygen density, $[N_O]$ (reciprocal of the glass volume per gram oxygen atom), the bulk modulus, K, and mean stretching force constants, F. There is no reason why this model should not be applicable to single relaxation processes of the same form, in which case n_1, n_2, C_1 and C_2 should be proportional to $N_O(F/K)$, whilst C_1 and C_2 should be proportional to (F/K). Indeed, Fig. 13 shows that

$$V_1 \approx \text{const}_1(F/K), \quad \text{correlation coefficient } 98\% \tag{11}$$

$$V_2 \approx \text{const}_2(F/K), \quad \text{correlation coefficient } 94\% \tag{12}$$

but correlation coefficients for the other relationships are poor and are not drawn, the best result being 59% for the n_1 against $[N_O](F/K)$ relation.

8. Frequency dependence of attenuation at constant temperature

By inspection of Figs 14a to d we note that at the peak temperature (~400 K for the R_1 process and ~600 K

for the R_2 process), the value of x in the equation

$$\alpha = \beta v^x \quad (13)$$

is about 1.0 in our Co–P–O glasses, consistent with a single relaxation process. On the high-temperature side of each peak, the value of x in Equation 13 decreases gradually from 1.0 to 0.8. However, for a truly single relaxation process, under such conditions, i.e. $\omega\tau < 1$, x should approach 2. On the low-temperature side of the peaks we find that the frequency dependence of the loss is similar to what happens on the high-temperature side. But for a single relaxation process, x should decrease much more rapidly, approaching 0 for $\omega\tau \gg 1$. The above discrepancies are presumably explicable in terms of (i) the overlap of the R_1 and R_2 single relaxation processes, (ii) for T sufficiently less than T_{P1} the low-temperature multiple relaxation process [1] eventually takes over tending to make $x \approx 1$ for constant T, (iii) for T sufficiently greater than T_{P2} departure from single relaxation behaviour is probably due to the fact that there exists a third loss peak (relating to viscous flow processes) in our glasses at temperatures higher than our measurement range.

9. Conclusion

The most interesting feature of high-temperature acoustic relaxation in CoO_3–P_2O_5 glasses is that the shape of the loss peaks can be explained in terms of discrete relaxation times, rather than by a distribution of times as required for the low-temperature loss. The observed activation energies are too low for the phenomenon to be explicable in terms of ionic diffusion, i.e. irreversible motion of individual atoms or groups of atoms through the network stemming from broken bonds. Equally, on the two-well model, the observed activation energies and attempt frequencies are generally too large and too small, respectively, for the relaxing particles to be single oxygen atoms moving in wells of dimensions of the order of an atomic spacing. The two well systems involved are thus different from those governing the low-temperature loss. However, the former and the latter do occur in approximately the same numbers and enjoy the same kind of correlation with the product of mean stretching force constant and compressibility.

References

1. B. BRIDGE and N. D. PATEL, *J. Mater. Sci.* **21** (1986) 3783.
2. A. A. HIGAZY and B. BRIDGE, *ibid.* **23** (1988) in press.
3. B. BRIDGE, *J. Mater. Sci. Lett.* **5** (1986) 1203.
4. B. BRIDGE and N. D. PATEL, *ibid.* **5** (1986) 1198.
5. E. PAPPADAKIS, *J. Acoust. Soc. Amer.* **42** (1967) 1045.
6. A. A. HIGAZY and B. BRIDGE, *J. Non-Crystall. Solids* **72** (1985) 81.
7. *Idem, Phys. Chem. Glasses* **26** (3) (1985) 82.
8. B. BRIDGE and A. A. HIGAZY, *J. Mater. Sci. Lett.*, submitted.
9. B. BRIDGE and N. D. PATEL, *ibid.* **5** (1986) 1255.

Received 9 February
and accepted 28 April 1987